

## Thermal-sizing of the molten salt reactor system with gas Brayton cycle

In Woo Son<sup>a</sup>, Sungwook Choi<sup>a</sup>, Sang Ji Kim<sup>b</sup>, Jeong Ik Lee<sup>a\*</sup>

<sup>a</sup>Dept. Nuclear & Quantum Eng., KAIST, 373-1, Guseong-dong, Yuseong-gu, Daejeon, 305-701, Republic of Korea

<sup>b</sup> Korea Atomic Energy Research Institute, 989-111 Daedeok-daero, Yuseong-gu, Daejeon, 34057, Korea

\*Corresponding author: jeongiklee@kaist.ac.kr

### 1. Introduction

The Molten Salt Reactor (MSR), one of the generation IV nuclear reactors, has recently received much attention worldwide due to its technology, safety, and economic feasibilities. MSRs have a high core power density, which is advantageous for compact system. A molten salt has generally lower chemical reactivity than liquid sodium and has high boiling point, so high-temperature operation is possible. In addition, since there is no cladding and solid nuclear fuel as well as fuel supporting structure in the core, neutron loss is small. It is also possible to add nuclear fuel and separate fission products during operation if it is needed. The reactor can operate at atmospheric pressure and maintain high safety by keeping the surplus reactivity low. Based on these advantages, all generation IV reactor international forum member countries are participating in the development of the MSR technology, and about 25 overseas start-up companies are developing the MSR concept design [1-4].

During the development of MSR design concepts, determining which power conversion system is suitable for the system is an important issue. Therefore, in this study, a power conversion system suitable for a small modular MSR is investigated. To design the power conversion system, thermal sizing of the entire MSR is first required, which is carried out by referring to the Molten Salt Reactor Experiment (MSRE) conducted at ORNL (*Oak Ridge National Laboratory*) [5]. However, as shown in Table 1, the MSRE system does not have a temperature range suitable for the efficient power production because the temperature difference between the fuel salt and the coolant salt of the primary side heat exchanger is quite large to reduce the heat exchanger size as well as cooling power.

Table 1. Primary Heat exchanger design parameter of the MSRE system [5]

|                                 | Shell side<br>(Fuel salt) | Tube side<br>(Coolant salt) |
|---------------------------------|---------------------------|-----------------------------|
| Inlet / Outlet temperature [°C] | 662.78 / 635              | 551.67 / 593.33             |
| Inlet / Outlet Pressure [kPa]   | 379.2 / 241.3             | 530.9 / 324.0               |
| Pressure drop [kPa]             | 165.47                    | 199.95                      |
| Mass Flow Rate [kg/sec]         | 163.31                    | 103.083                     |

Therefore, the objectives of this study are as follows: 1. Reconfiguration and thermal-sizing of MSRE system suitable for power production. 2: Selection of a suitable power conversion cycle for the modeled MSRE system.

### 2. Methods and Results

In this study, the primary and intermediate loops suitable for the power conversion system are modeled as shown in Fig. 1. The fuel salt is assumed to be based on NaCl-MgCl<sub>2</sub> because chlorine salt can dissolve major radioactive substances such as Cs, Sr, and I. These chemical properties prevent the leakage of radioactive materials when fuel salt is leaked to the outside. The design parameters of the primary side are selected as shown in Table 2 using the heat output and the fuel salt mass flow rate of the MSRE [5]. The effectiveness values of both primary and secondary heat exchangers are assumed to be 90%, and the difference between the hot side inlet temperature and the cold side outlet temperature is selected as 10K. The PCHE type primary heat exchanger is conceptually designed using the KAIST-HXD (Heat eXchanger Design) code, and the used thermal properties and correlation are summarized in Table 3 [6, 7]. The KAIST-HXD code is a MATLAB-based 1D-FDM in-house code, and detailed description and validation process are shown in the reference [8]. As a result, the primary heat exchanger could be designed by adjusting the relationship between the length of the heat exchanger and the pressure drop as shown in Table 4.

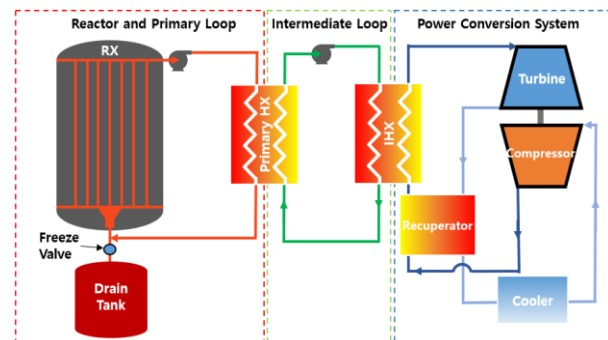


Fig. 1. The modeled MSRE system with power conversion system

Table 2. Primary heat exchanger design parameter of the modeled MSRE system

| Primary Heat exchanger design parameter |
|---|
|---|

|   |                 |
|---|-----------------|
| Heat load   | 10MWth [5]      |
| Hot side mass flow rate                             | 163.31 kg/s [5] |
| Hot side inlet temp.                                | 650°C           |
| Effectiveness                                       | 90%             |
| $\Delta T_{\text{hot side inlet-cold side outlet}}$ | 10 K            |

Table 3. Thermal property and heat exchanger correlation of the NaCl-MgCl<sub>2</sub>

|  |  |
|--|--|
| <b>Thermal property [6]</b>  |  |
| $C_p = 1.08019 \times 1000 \left[ \frac{J}{kg \cdot K} \right]$  |  |
| $\rho = (2.2971 - 0.000507 \times (T - 273.15)) \times 1000 \left[ \frac{kg}{m^3} \right]$                           |  |
| $\mu = \left( 0.0286 \times \exp\left(\frac{1441}{T}\right) \right) \times 0.01 \left[ \frac{kg}{m \cdot s} \right]$ |  |
| $k = 0.000267 \times (T - 273.15) + 0.3133 \left[ \frac{W}{m \cdot K} \right]$                                       |  |
| <b>Heat exchanger Correlation [7]</b>  |  |
| $Nu = 4.089$ (Laminar flow)  |  |
| $f = 15.78/Re$ (Laminar flow)  |  |

Table 4. The Primary heat exchanger design results

| Design parameter                | Cold side pressure drop = 30kPa | Cold side pressure drop = 50kPa | Cold side pressure drop = 100kPa |
|---------------------------------|---------------------------------|---------------------------------|----------------------------------|
| HX length (m)                   | 2.36                            | 3.05                            | 4.32                             |
| Hot side outlet temp (K)        | 593.32                          | 587.01                          | 593.32                           |
| Cold side outlet temp (K)       | 587.01                          | 587.01                          | 587.01                           |
| Hot side pressure drop (kPa)    | 26                              | 46                              | 92                               |
| Hot side Average Re             | 648                             | 836                             | 1183                             |
| Cold side Average Re            | 683                             | 882                             | 1247                             |
| Cold side mass flow rate (kg/s) | 174.72                          | 174.72                          | 174.72                           |
| HX Volume                       | 3.27                            | 3.27                            | 3.27                             |

To design an intermediate heat exchanger connecting the secondary and tertiary sides, the mass flow rate of the power conversion system should be calculated first. In the operating temperature range (550-630°C), the cycle with good efficiency while having high compactness is the gas Brayton cycle [9]. Therefore, an air open Brayton recuperated cycle and an sCO<sub>2</sub> (Supercritical CO<sub>2</sub>) closed Brayton recuperated cycle are designed and compared in this study. The difference between the hot side inlet temperature and the cold side outlet temperature of the intermediate heat exchanger is selected as 10K. The design parameters of each cycle are assumed as shown in Tables 5 and 6 by referring values from the previous works [10-14]. The cycle optimization variable is the turbine pressure ratio, and the optimization target is the maximum of cycle thermal efficiency and cycle-specific work product.

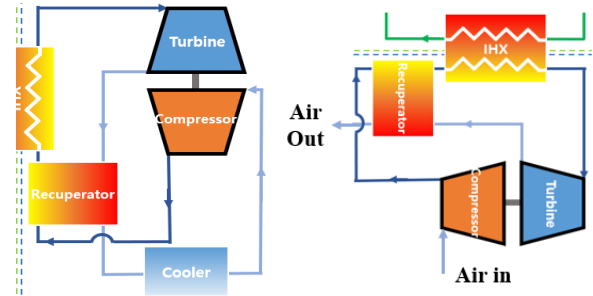


Fig. 2. (a) sCO<sub>2</sub> recuperated power Brayton closed cycle (b) Air recuperated power Brayton open cycle

Table 5. Design parameters of the sCO<sub>2</sub> power conversion system [10, 11]

|                                |                     |
|--------------------------------|---------------------|
| Max Pressure                   | 20 – 25 Mpa         |
| Min Temperature                | 60°C                |
| Max Temperature                | 630°C               |
| Thermal heat                   | 10 MW <sub>th</sub> |
| Turbine efficiency             | 90%                 |
| Compressor efficiency          | 86%                 |
| Recuperator effectiveness      | 0.92                |
| <b>Component pressure drop</b> | <b>100-250 kPa</b>  |
| Heater Cold side               | 150 kPa             |
| Recuperator Hot side           | 250 kPa             |
| Recuperator Cold side          | 100 kPa             |
| Cooler Hot side                | 100 kPa             |

Table 6. Design parameters of the Air power conversion system [12-14]

|   |                     |
|---|---------------------|
| Min Temperature                         | 15 / 25 / 60°C      |
| Max Temperature                         | 630°C               |
| Thermal heat                            | 10 MW <sub>th</sub> |
| Compressor inlet Pressure               | 101.325 kPa         |
| Turbine efficiency                      | 90%                 |
| Compressor efficiency                   | 86%                 |
| Recuperator effectiveness               | 0.92                |
| <b>Component pressure Ratio</b>         | <b>-</b>            |
| Heater Cold side                        | 0.01                |
| Recuperator Hot side                    | 0.01                |
| Recuperator Cold side                   | 0.01                |
| Ratio of exhaust pressure to atmosphere | 0.98                |

Cycle optimization is performed through KAIST-CCD (Closed Cycle Design) and KAIST-OCD (Open Cycle Design) codes. Algorithms of KAIST-CCD code and KAIST-OCD code are shown in the figure below, respectively [15]. Cycle optimization results are calculated in Tables 7 and 8, respectively.

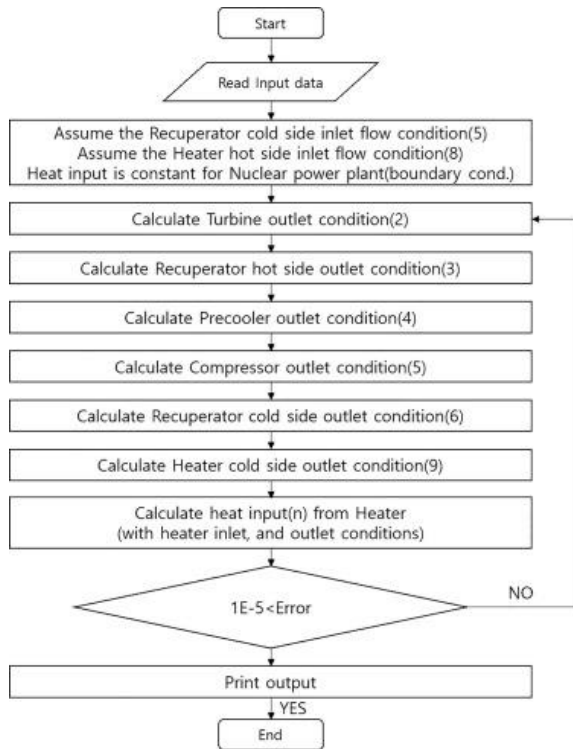


Fig. 3. Algorithms of KAIST-CCD code

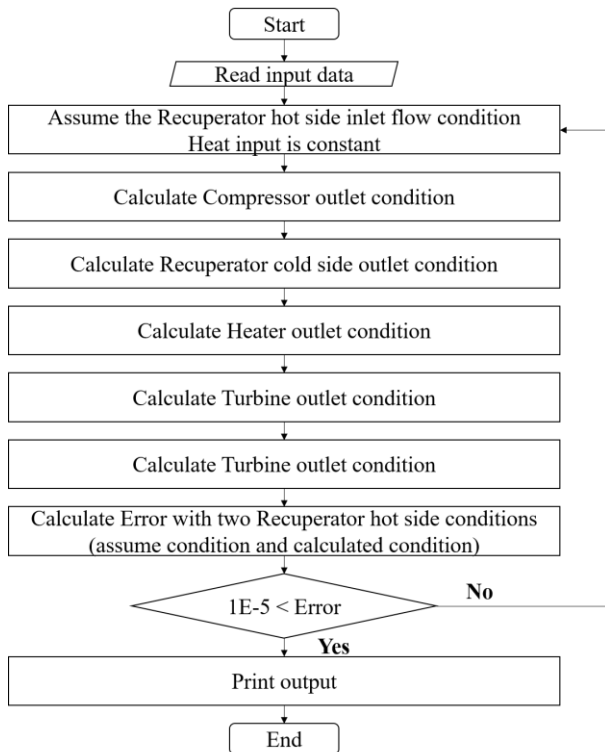


Fig. 4. Algorithms of KAIST-OCD code

Table 7. Cycle optimization results of the sCO<sub>2</sub> cycle

| Design parameter                    | sCO <sub>2</sub><br>Max pres. =<br>20MPa | sCO <sub>2</sub><br>Max pres. =<br>25MPa |
|-------------------------------------|--|--|
| Cycle Thermal efficiency (%)        | 32.99                                    | 34.13                                    |
| Cycle work (MW <sub>e</sub> )       | 3.30                                     | 3.41                                     |
| Specific Work (MW <sub>e</sub> /kg) | 0.086                                    | 0.093                                    |
| Thermal heat (MW <sub>th</sub> )    | 10                                       | 10                                       |
| Pressure ratio                      | 3.59                                     | 3.54                                     |
| Min. Pressure (MPa)                 | 5.16                                     | 6.63                                     |
| Mass flow rate (kg/s)               | 38.59                                    | 36.82                                    |

| Design parameter                    | Air<br>Min Temp. =<br>60 °C | Air<br>Min Temp. =<br>25 °C | Air<br>Min Temp. =<br>15 °C |
|-------------------------------------|-----------------------------|-----------------------------|-----------------------------|
| Cycle Thermal efficiency (%)        | 29.94                       | 34.59                       | 35.94                       |
| Cycle work (MW <sub>e</sub> )       | 2.99                        | 3.46                        | 3.59                        |
| Specific Work (MW <sub>e</sub> /kg) | 0.072                       | 0.092                       | 0.099                       |
| Thermal heat (MW <sub>th</sub> )    | 10                          | 10                          | 10                          |
| Pressure ratio                      | 2.95                        | 3.45                        | 3.63                        |
| Max. Pressure (MPa)                 | 0.31                        | 0.37                        | 0.39                        |
| Mass flow rate (kg/s)               | 41.80                       | 37.54                       | 36.42                       |

Table 8. Cycle optimization results of the air cycle

|                                     |       |       |       |
|-------------------------------------|-------|-------|-------|
| Cycle Thermal efficiency (%)        | 32.99 | 34.13 | 34.13 |
| Cycle work (MW <sub>e</sub> )       | 3.30  | 3.41  | 3.41  |
| Specific Work (MW <sub>e</sub> /kg) | 0.086 | 0.093 | 0.093 |
| Thermal heat (MW <sub>th</sub> )    | 10    | 10    | 10    |
| Pressure ratio                      | 3.59  | 3.54  | 3.54  |
| Min. Pressure (MPa)                 | 5.16  | 6.63  | 6.63  |
| Mass flow rate (kg/s)               | 38.59 | 36.82 | 36.82 |

As a result, it can be seen that the air power cycle has relatively high thermal efficiency and specific work compared to the sCO<sub>2</sub> closed Brayton cycle. For the sCO<sub>2</sub> cycle, it was confirmed that the cycle maximum pressure did not significantly affect the cycle efficiency. In addition, due to the limitation of the indirect air-cooling method, the minimum temperature was fixed at 60°C, so it did not show the best power cycle performance compared to the air cycle in this case. On the other hand, since the air cycle is an open Brayton cycle, it was able to have a lower minimum temperature compared to the sCO<sub>2</sub> cycle. Therefore, the air power cycle showed competitive thermal performance with the sCO<sub>2</sub> power cycle for the lowest air temperature case. It is noted that the sCO<sub>2</sub> cycle efficiency can be further improved by adding a recompression process, but this option is not explored in this study since minimizing reactor system weight and volume is also a key for small modular reactor type concept development.

### 3. Conclusions

A thermal sizing of MSR system is conducted in this study for efficient power production. As a result of the conceptual design, the maximum temperature of the power conversion system can reach up to 630°C, and the air open Brayton cycle and the sCO<sub>2</sub> closed Brayton cycle are optimized and compared. As a result, it is confirmed that the air open Brayton power cycle has comparable thermal efficiency and specific work with the sCO<sub>2</sub> closed Brayton power cycle. Considering volume and weight of the system, the air open Brayton

cycle is selected as a power conversion system for the MSR system, and the intermediate heat exchanger connecting the secondary and tertiary sides will be conceptually designed further.

### ACKNOWLEDGEMENTS

This work was supported by the National Research Foundation of Korea (NRF) grant funded by the Korea government (MSIP) (2017M2B2B1071971)

### REFERENCES

- [1] Jorgensen, Lars. "ThorCon reactor." *Molten Salt Reactors and Thorium Energy*. Woodhead Publishing, 2017. 557-564.
- [2] Sowder, A. "Program on Technology Innovation: Technology Assessment of a Molten Salt Reactor Design—The Liquid-Fluoride Thorium Reactor (LFTR)." *Electric Power Research Institute* (2015).
- [3] Choe, J., et al. "Fuel Cycle Flexibility of Terrestrial Energy's Integral Molten Salt Reactor (IMSR)." *38th Annual Conference of the Canadian Nuclear Society and 42nd Annual CNS/CNA Student Conference, Saskatoon, SK, Canada, June*. 2018.
- [4] Dolan, Thomas James, ed. *Molten salt reactors and thorium energy*. Woodhead Publishing, 2017.
- [5] Robertson, R. C. "MSRE design and operations report part I: description of reactor design." *ORNL-TM-728, Oak Ridge National Laboratory* (1965).
- [6] Williams, D. F. *Assessment of candidate molten salt coolants for the NNGP/NHI heat-transfer loop*. No. ORNL/TM-2006/69. Oak Ridge National Lab.(ORNL), Oak Ridge, TN (United States), 2006.
- [7] Hesselgreaves, John E., Richard Law, and David Reay. *Compact heat exchangers: selection, design and operation*. Butterworth-Heinemann, 2016.
- [8] Baik, Seungjoon, et al. "Study on CO<sub>2</sub>-water printed circuit heat exchanger performance operating under various CO<sub>2</sub> phases for S-CO<sub>2</sub> power cycle application." *Applied Thermal Engineering* 113 (2017): 1536-1546.
- [9] Ahn, Yoonhan, et al. "Review of supercritical CO<sub>2</sub> power cycle technology and current status of research and development." *Nuclear engineering and technology* 47.6 (2015): 647-661.
- [10] Binotti, Marco, et al. "Preliminary assessment of sCO<sub>2</sub> cycles for power generation in CSP solar tower plants." *Applied energy* 204 (2017): 1007-1017.
- [11] Le Moullec, Yann, et al. "Shouhang-EDF 10MWe supercritical CO<sub>2</sub> cycle+ CSP demonstration project." *3rd European Conference on Supercritical CO<sub>2</sub> (sCO<sub>2</sub>) Power Systems 2019: 19th-20th September 2019*.
- [12] Kays, William Morrow, and Alexander Louis London. "Compact heat exchangers." (1984).
- [13] Zohuri, Bahman, Pat McDaniel, and Cassiano de Oliveira. "High Temperature Recuperated Open Air

Brayton Cycle for the Next Open Air Brayton Cycle for the Next Generation Nuclear Plant."

[14] Zohuri, Bahman. *Innovative open air Brayton combined cycle systems for the next generation nuclear power plants*. The University of New Mexico, 2014.

[15] Son, In Woo, et al. "Feasibility study of solar-nuclear hybrid system for distributed power source." *Energy Conversion and Management* 230 (2021): 113808.